



OUTPUT-ONLY MODAL IDENTIFICATION BASED ON WAVELET-BASED TEMPORAL PREDICTABILITY

C. S. Huang⁽¹⁾, G. P. Lee⁽²⁾, C. Y. Huang⁽³⁾, W. C. Su⁽⁴⁾

⁽¹⁾ Professor, National Chiao Tung University, Taiwan, cshuang@mail.nctu.edu.tw

⁽²⁾ Graduate Student, National Chiao Tung University, Taiwan, amylee6232@gmail.com

⁽³⁾ Graduate Student, National Chiao Tung University, Taiwan, 0975782695x@gmail.com

⁽⁴⁾ Associate Researcher, National Center for High Performance Computing, Taiwan, wichcv86@gmail.com

Abstract

Modal parameters of a structure identified from its measured dynamic responses can offer a valuable reference to efforts to update structural design models and perform vibration control, health monitoring and damage assessment of the structure. This study presents a novel blind source separation (BSS) approach to accurately identify modal parameters of a linear system with classical damping under non-stationary input from its output-only measurements and demonstrates the applications to a steel frame under shaking table tests. The proposed approach employs the temporal predictability of the continuous wavelet transforms of responses to estimate the modal vectors of a structure and to obtain its modal responses in wavelet domain. The modal damping ratios and natural frequencies are further estimated from the Fourier spectra of modal responses. Notably, the existing BSS approaches typically require the number of measured degrees of freedom of a structure equal to the number of modes to be identified. The proposed approach does not have such requirement by using the filtering properties of the wavelet transform. The efficiency of the proposed approach is first validated using numerically simulated acceleration responses of a six-story shear building subjected to earthquake base excitations with considering the effects of noise and incomplete measurements. The band-filter-like real Shannon wavelets are utilized in this study. Finally, the proposed approach is further employed to process the acceleration responses of an eight-story steel frame under shaking table tests to show the applicability of the proposed approach to engineering practices. The identified modal parameters are compared with those obtained from autoregressive with exogenous input models with the continuous Cauchy wavelet transform to confirm the accuracy.

Keywords: blind source separation; temporal predictability; continuous wavelet transform; modal parameter identification; output-only earthquake responses



1. Introduction

Failure of civil infrastructure due to severe loading, such as a strong earthquake, or degradation of material can cause substantial societal and human consequence. Identification of modal parameters of a structure from its earthquake responses and ambient vibration responses is important to carry out the damage assessment of the structure. The input base excitations or forces to a structure may not be all measurable because of the difficulties of identifying or measuring the input forces (i.e., considering soil-structure interaction under an earthquake or too many possible input forces in ambient vibrations). Additionally, the cost in establishing a structural health monitoring system is less without measuring the inputs. Consequently, it is a challenging and important task to identify the modal parameters of a structure from its measured responses only.

A vast number of output-only approaches have been published based on the concept of blind source separation (BSS), which assumes that observed signals are linear combinations of source signals. The modal decomposition expression of the dynamic responses of a linear structure fits the mathematic model of BSS. The most popular BSS algorithms can be categorized into three classes: independent component analysis (ICA) [1-3], second-order blind identification (SOBI) [4-6], and sparse component analysis (SCA) [7,8]. ICA assumes that the source signals are statistically independent and have non-Gaussian distributions. Hyvärinen and Oja [9] provided a solid theoretical background behind ICA and introduced measures of non-Gaussianity, including fourth-order cumulant and negentropy. A time-domain ICA is typically limited to weakly damped systems and strongly affected by noise in the data [10,11]. Yang and Nagarajaiah [2] proposed a time-frequency-domain ICA to improve these shortcomings by using a short-time Fourier transform. SOBI assumes that the source signals are statistically uncorrelated. Morovati and Kazemi [5] introduced a time-frequency-domain SOBI to enhance the capability of a time-domain SOBI in processing seismic data and identifying modal parameters of closely spaced modes and highly damped modes. McNeil [12] combined Hilbert transform with SOBI to process the responses of nonclassical damping structural systems. Hazra and Narasimhan [13] employed SOBI with stationary wavelet transform to process the ambient vibrations responses and earthquake responses of a building. SCA assumes that the source signals can be sparsely represented in a transformed domain. Different transforms, including discrete cosine transform [14], short-time Fourier transform [15], and quadratic time-frequency analysis, and different clustering algorithms with various norms [7] have resulted in different SCA-based techniques.

The study is to explore the applicability of the BSS approach using temporal predictability proposed by Stone [16, 17] to identify the mode shapes and modal responses of a linear structural system with classical damping under earthquake base excitations. To overcome the drawbacks of most BSS approaches that identify less active modes than the number of measured degrees of freedom, the continuous wavelet transform is applied to measured responses of a structure, and the modal vectors and modal responses of the structure are estimated in wavelet domain via reformulated Stone's measure of the temporal predictability in wavelet domain. Then, the natural frequencies and modal damping ratios are identified from the Fourier spectra of modal responses. The validity of the proposed approach is first confirmed through processing the numerically simulated absolute acceleration responses of a six-story shear building subjected to an earthquake with considering the effects of noise and incomplete measurements. Then, the present approach is further applied to identify the modal parameters of an eight-story steel frame under shaking table tests.

2. Methodology

The BSS approaches are based on the model

$$\hat{\mathbf{x}}(t) = \mathbf{A}\mathbf{s}(t), \quad (1)$$

where $\hat{\mathbf{x}}(t)$ and $\mathbf{s}(t)$ denote column vectors of observed signals and source signals, respectively, and \mathbf{A} is constant matrix. Based on statistically independent source signals, Stone [16] adopted the conjecture that the temporal predictability of any signal mixture is less than that of any of its



component source signals and proposed a measure of temporal predictability to determine \mathbf{A} and $\mathbf{s}(t)$ in time domain. Such approach requires that the dimension of $\hat{\mathbf{x}}(t)$ is the same as that of $\mathbf{s}(t)$.

The form of Eq. (1) is exactly the same as that for the modal decomposition of dynamic responses, $\mathbf{x}(t)$, of a linear structure,

$$\mathbf{x}(t) = \mathbf{\Phi} \mathbf{q}(t) = \sum_{i=1}^N q_i(t) \boldsymbol{\phi}_i, \quad (2)$$

where $\mathbf{\Phi}$ is the modal vector matrix of the structure with N degrees of freedom; $\boldsymbol{\phi}_i$ is the i^{th} column of $\mathbf{\Phi}$; $\mathbf{q} = (q_1, q_2, \dots, q_N)^T$, and $q_i(t)$ is the modal response function corresponding to the i^{th} mode $\boldsymbol{\phi}_i$. Notably, \mathbf{x} and \mathbf{q} can be acceleration, velocity or displacement. In real applications, incomplete measurements are always encountered, and more modes than the measured degrees of freedom are wanted to identify, which forms underdetermined output-only problems. Consequently, Eq. (2) is reformed as

$$\mathbf{y}(t) = \bar{\mathbf{\Phi}} \mathbf{q}(t) = \sum_{i=1}^N q_i(t) \bar{\boldsymbol{\phi}}_i, \quad (3)$$

where \mathbf{y} denotes the vector of responses of measured degrees of freedom, and $\bar{\mathbf{\Phi}}$, sub-matrix of $\mathbf{\Phi}$, is modal vector matrix corresponding to the measured degrees of freedom. To fit the needs in real applications, the continuous wavelet transform is introduced into Stone's approach to filter out the unwanted frequency components of the responses for identifying wanted modal vectors and modal responses.

The continuous wavelet transform (CWT) has provided a popular time-frequency domain analysis technique. The continuous wavelet transform of a function of time, $f(t)$, belonging to L^2 space, is defined as

$$W_{\psi}(\bar{a}, b) \{f(t)\} \equiv |\bar{a}|^{-1/2} \int_{-\infty}^{\infty} f(t) \psi^* \left(\frac{t-b}{\bar{a}} \right) dt, \quad (4)$$

where the superscript $*$ denotes the complex conjugate; \bar{a} is a scale parameter, which is typically a positive real and plays the role of the inverse of frequency; b is a translation parameter, which indicates the locality of the transformation, and $\psi(t)$ is a mother wavelet function. Applying CWT to Eq. (3) and using the filtering properties of CWT yield

$$\mathbf{Y}(\bar{a}, b) \approx \sum_{i=k}^{k+\bar{N}} Q_i(\bar{a}, b) \bar{\boldsymbol{\phi}}_i, \quad (5)$$

where $\mathbf{Y}(\bar{a}, b) = W_{\psi}(\bar{a}, b) \{\mathbf{y}(t)\}$ and $Q_i(\bar{a}, b) \equiv W_{\psi}(\bar{a}, b) \{q_i(t)\}$. The CWT is applied to the responses to preserve the frequency components of the responses between natural frequencies of k^{th} and $(k + \bar{N})^{\text{th}}$ modes. Equation (5) can be rewritten as

$$\mathbf{Q}(\bar{a}, b) = \hat{\mathbf{\Phi}}^{-1} \mathbf{Y}(\bar{a}, b) = \mathbf{W}^T \mathbf{Y}(\bar{a}, b), \quad (6)$$

where $\mathbf{Q}(\bar{a}, b) = (Q_k(\bar{a}, b) \quad Q_{k+1}(\bar{a}, b) \quad \dots \quad Q_{k+\bar{N}}(\bar{a}, b))^T$ and $\hat{\mathbf{\Phi}} = [\bar{\boldsymbol{\phi}}_k \quad \bar{\boldsymbol{\phi}}_{k+1} \quad \dots \quad \bar{\boldsymbol{\phi}}_{k+\bar{N}}]$.

Redefine the measure of temporal predictability, denoted by TP, proposed by Stone [16] in wavelet domain as



$$TP(Q_i(\bar{a}, b)) = \log \frac{\sum_{j=1}^n (\bar{Q}_i(\bar{a}, b_j) - Q_i(\bar{a}, b_j))^2}{\sum_{j=1}^n \hat{Q}_i((\bar{a}, b_j) - Q_i(\bar{a}, b_j))^2} = \log \frac{\bar{V}_i}{\hat{V}_i}, \quad (7)$$

where \bar{Q}_i and \hat{Q}_i are long-term and short-term predictors of Q_i , respectively, and are given by

$$\bar{Q}_i(\bar{a}, b_j) = \lambda_L \bar{Q}_i(\bar{a}, b_{j-1}) + (1 - \lambda_L) Q_i(\bar{a}, b_{j-1}), \quad (8)$$

$$\hat{Q}_i(\bar{a}, b_j) = \lambda_s \hat{Q}_i(\bar{a}, b_{j-1}) + (1 - \lambda_s) Q_i(\bar{a}, b_{j-1}), \quad (9)$$

$$\lambda_\gamma = 2^{-1/h_\gamma}, \quad (10)$$

h_s is typically set equal to 1 and h_L is sufficient larger than h_s . The present study sets $h_L = 900000$, which was used in Yang and Nagarajaiah [18]. Incorporating Eq. (6) into (7) leads to

$$TP(Q_i(\bar{a}, b)) = \log \frac{(\mathbf{w}_i)^T \bar{\mathbf{R}} \mathbf{w}_i}{(\mathbf{w}_i)^T \hat{\mathbf{R}} \mathbf{w}_i}, \quad (11)$$

where \mathbf{w}_i is the i^{th} column of \mathbf{W} ; the (i, j) components of $\bar{\mathbf{R}}$ and $\hat{\mathbf{R}}$ are, respectively,

$$\bar{r}_{ij} = \sum_{k=1}^n (Y_i(\bar{a}, b_k) - \bar{Y}_i(\bar{a}, b_k)) (Y_j(\bar{a}, b_k) - \bar{Y}_j(\bar{a}, b_k)), \quad (12)$$

$$\hat{r}_{ij} = \sum_{k=1}^n (Y_i(\bar{a}, b_k) - \hat{Y}_i(\bar{a}, b_k)) (Y_j(\bar{a}, b_k) - \hat{Y}_j(\bar{a}, b_k)), \quad (13)$$

$$\bar{Y}_i(\bar{a}, b_j) = \lambda_L \bar{Y}_i(\bar{a}, b_{j-1}) + (1 - \lambda_L) Y_i(\bar{a}, b_{j-1}), \quad (14)$$

$$\hat{Y}_i(\bar{a}, b_j) = \lambda_s \hat{Y}_i(\bar{a}, b_{j-1}) + (1 - \lambda_s) Y_i(\bar{a}, b_{j-1}). \quad (15)$$

Maximizing TP yields

$$\nabla_{(\mathbf{w}_i)} TP(Q_i(\bar{a}, b)) = \mathbf{0}. \quad (16)$$

Substituting Eq. (11) into Eq. (16) gives

$$\frac{2(\mathbf{w}_i)^T \bar{\mathbf{R}}}{\bar{V}_i} - \frac{2(\mathbf{w}_i)^T \hat{\mathbf{R}}}{\hat{V}_i} = \mathbf{0}. \quad (17)$$

Equation (17) is rewritten as

$$\bar{\mathbf{R}}^T \mathbf{w}_i = \frac{\bar{V}_i}{\hat{V}_i} \hat{\mathbf{R}}^T \mathbf{w}_i, \quad (18)$$

which presents an eigenvalue problem, and \mathbf{w}_i can be easily determined.

After \mathbf{w}_i are determined, the modal eigenvector matrix corresponding to the measured degrees of freedom is determined by $\hat{\Phi} = \mathbf{W}^{-T}$, then the modal responses in wavelet domain $\mathbf{Q}(\bar{a}, b)$ are found through Eq. (6). The modal assurance criterion (MAC) [19], given Eq. (19), is applied to verify the agreement between the identified ($\bar{\phi}_{il}$) and theoretical ($\bar{\phi}_{iT}$) mode shapes,



$$\text{MAC} = \frac{|\bar{\Phi}_{iT}^T \bar{\Phi}_{iT}|^2}{\bar{\Phi}_{iT}^T \bar{\Phi}_{iT} \bar{\Phi}_{iT}^T \bar{\Phi}_{iT}}. \quad (19)$$

After $Q_i(\bar{a}, b)$ is found, the natural frequency and modal damping ratio of the i^{th} mode are simply estimated in frequency domain. Following Eq. (4) gives

$$Q_i(\bar{a}, b) = |\bar{a}|^{-1/2} \int_{-\infty}^{\infty} q_i(t) \psi^* \left(\frac{t-b}{\bar{a}} \right) dt. \quad (20)$$

Applying Fourier transform to Eq. (20) gives

$$|\tilde{Q}_i(\bar{a}, \omega)| = \sqrt{\bar{a}} |\tilde{\psi}(\bar{a}\omega)| |\tilde{q}_i(\omega)|, \quad (21)$$

where $\tilde{Q}_k(\bar{a}, \omega) = \int_{-\infty}^{\infty} Q_k(\bar{a}, b) e^{-i\omega b} db$, $\tilde{\psi}(\bar{a}\omega) = \int_{-\infty}^{\infty} \psi(\tau) e^{-i\bar{a}\omega\tau} d\tau$ and $\tilde{q}_k(\omega) = \int_{-\infty}^{\infty} q_k(t) e^{-i\omega t} dt$. Hence,

$$|\tilde{q}_i(\omega)| = \frac{|\tilde{Q}_i(\bar{a}, \omega)|}{\sqrt{\bar{a}} |\tilde{\psi}(\bar{a}\omega)|}. \quad (22)$$

When $q_k(t)$ represents modal acceleration responses, structural dynamics gives

$$|\tilde{q}_k(\omega)| = \frac{\omega^2 |\tilde{g}_k(\omega)|}{|-\omega^2 + 2i\bar{\xi}_k \bar{\omega}_k \omega + \bar{\omega}_k^2|}, \quad (23)$$

where $\tilde{g}_k(\omega)$ represents the Fourier transform of external force corresponding to k^{th} mode, and $\bar{\omega}_k$ and $\bar{\xi}_k$ are the natural frequency and modal damping ratio of k^{th} mode, respectively. Equation (23) indicates that if $|\tilde{g}_k(\omega)|$ does not have sharp peaks, which typically happens in earthquake inputs, there should be only one sharp peak in $|\tilde{q}_k(\omega)|$. Using Eqs. (22) and (23), one obtains

$$\frac{|\tilde{Q}_k(\bar{a}, \omega_{j+1})|}{|\tilde{Q}_k(\bar{a}, \omega_j)|} = \frac{|\tilde{\psi}(\bar{a}\omega_{j+1})|}{|\tilde{\psi}(\bar{a}\omega_j)|} \frac{\omega_{j+1}^2 |\tilde{g}_k(\omega_{j+1})|}{\omega_j^2 |\tilde{g}_k(\omega_j)|} \frac{|-\omega_j^2 + 2i\bar{\xi}_k \bar{\omega}_k \omega_j + \bar{\omega}_k^2|}{|-\omega_{j+1}^2 + 2i\bar{\xi}_k \bar{\omega}_k \omega_{j+1} + \bar{\omega}_k^2|} \quad (24)$$

Since the external forces are not measured, it is assumed that the external forces are piecewise constants in frequency domain, and $|\tilde{g}_k(\omega_j)| = |\tilde{g}_k(\omega_{j+1})|$ in Eq. (24). To find $\bar{\omega}_k$ and $\bar{\xi}_k$ from the Fourier spectrum $|\tilde{Q}_k(\bar{a}, \omega)|$, an error function is defined as follows,

$$E = \sum_j \left(\frac{|\tilde{Q}_k(\bar{a}, \omega_{j+1})|}{|\tilde{Q}_k(\bar{a}, \omega_j)|} - \frac{|\tilde{\psi}(\bar{a}\omega_{j+1})|}{|\tilde{\psi}(\bar{a}\omega_j)|} \frac{\omega_{j+1}^2}{\omega_j^2} \frac{|-\omega_j^2 + 2i\bar{\xi}_k \bar{\omega}_k \omega_j + \bar{\omega}_k^2|}{|-\omega_{j+1}^2 + 2i\bar{\xi}_k \bar{\omega}_k \omega_{j+1} + \bar{\omega}_k^2|} \right)^2. \quad (25)$$

The data points with ω_j between $0.95\omega_p$ and $1.05\omega_p$ and $|\tilde{Q}_k(\bar{a}, \omega_j)|$ between $0.5\text{Max}(|\tilde{Q}_k(\bar{a}, \omega)|)$ and $\text{Max}(|\tilde{Q}_k(\bar{a}, \omega)|)$, where ω_p is the frequency corresponding to $\text{Max}(|\tilde{Q}_k(\bar{a}, \omega)|)$, are used to construct Eq. (25). A typical genetic approach in MATLAB was employed to find $\bar{\omega}_k$ and $\bar{\xi}_k$, which minimizes the error function in Eq. (25).

In the present study, real Shannon wavelets were chosen for the CWT. The wavelets are defined as



$$\psi(t) = \sqrt{F_b} \cdot \text{sinc}(F_b \cdot t) \cdot \cos(2\pi F_c \cdot t), \quad (26)$$

where $\text{sinc}(t) = \sin(\pi t) / \pi t$. The wavelet is like a perfect band-pass filter with center at F_c and bandwidth equal to F_b .

3. Numerical Verification

The accuracy and effectiveness of the proposed approach in identifying modal parameters are verified by processing numerically simulated absolute acceleration responses of a six-story shear building subjected to earthquake base excitations. Each floor of the shear building has a mass of 1 ton, and the stiffness of 1st to 6th stories are 2000, 1500, 1100, 800, 600 and 500 KN/m, respectively. The damping matrix is set equal to $0.5\mathbf{M}$ 1/s, where \mathbf{M} is the mass matrix of the system. The Runge-Kutta method was applied herein to determine the dynamic responses of the shear building with a time increment of 0.004 s. The theoretical natural frequencies of the system were 1.31, 3.35, 5.25, 6.78, 8.42 and 11.02 Hz, and the modal damping ratios were 3.04%, 1.19%, 0.76%, 1.59%, 0.47%, 0.36%.

To simulate the situations encountered in real applications, the absolute acceleration responses of the 1st, 3rd and 6th floors with 10% variance of the signal-to-noise ratio were considered in the following analyses. Figure 1 depicts the earthquake base excitations and the absolute accelerations responses and the corresponding spectra of 1st, 3rd and 6th floors. The natural frequencies can be roughly estimated from the spectra.

To identify the modal parameters of the first three modes, the Shannon wavelet with $F_c=3.5$ and $F_b=5$ was used, and the responses with frequency band [1, 6] Hz were preserved in wavelet domain. The present approach gave the modal responses and the corresponding Fourier spectra shown in Fig. 2, while Fig. 3 shows the estimated results for the 4th to 6th modes using filtering band [6, 12]Hz. Each of the spectra shown in Fig. 2 has only one clear peak, which indicates that the modal vectors corresponding to these modal responses are reliable. The MAC values for the first to third modes are 0.996, 0.917, and 0.991, respectively. The natural frequencies and modal damping ratios estimated from those spectra are given in Table 1.

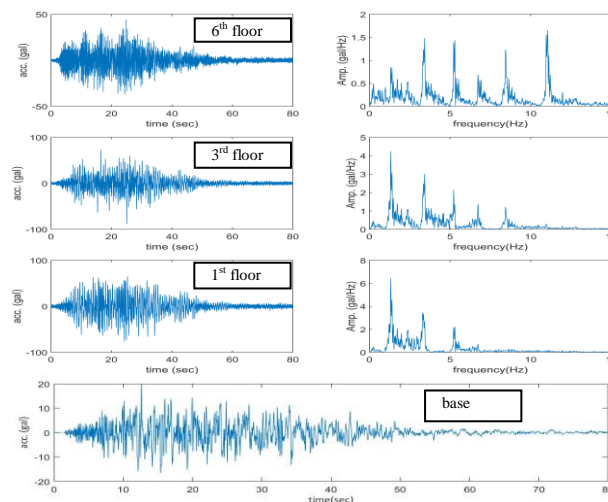


Fig. 1 Base excitations and the absolute accelerations responses and the corresponding spectra of 1st, 3rd and 6th floors

Each of the spectra in Fig. 3 has multiple peaks and is not corresponding to a single mode even though the spectrum in Fig. 3(a) looks like that for a single mode. The results in Fig. 3 are not satisfactory, and the



MAC values for the identified vectors corresponding to Figs. 3(a) to (c) are 0.944, 0.588 and 0.684, respectively. To find better results, the responses through CWT using Shannon wavelets with $(F_c, F_b) = (7.5, 3)$ and $(9.5, 4)$ were separately processed. The obtained modal responses and corresponding Fourier spectra are given in Figs. 4 and 5. Apparently, those spectra reveal that the modal responses in Figs. 4(a) and (b) are satisfactory for the 4th and 5th modes, respectively, while the modal responses in Figs. 5(a) and (b) are good for the 5th and 6th modes, respectively. The responses in Figs. 4(c) and 5(c) are corresponding to spurious modes. The MAC values of the identified modal vectors corresponding to the responses given in Figs. 4(a) and (b) are 0.954 and 0.998, respectively, while they are 0.987 and 0.999 for the identified vectors corresponding to responses in Figs. 5(a) and (b), respectively. The spectra in Figs. 4(a), 4(b), 5(a) and 5(b) were further used to identify natural frequencies and modal damping ratios, which are shown in Table 1.

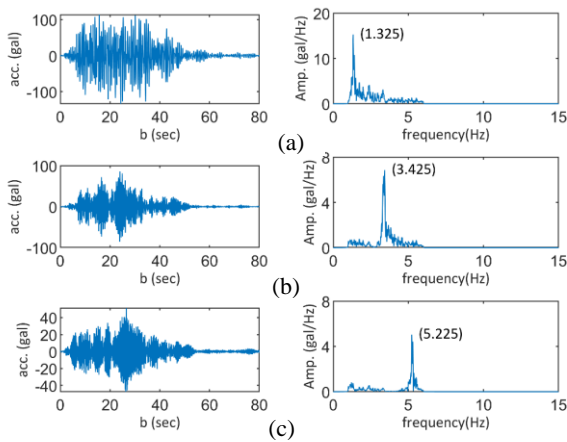


Fig. 2 The identified modal responses and spectra from responses with [1, 6]Hz

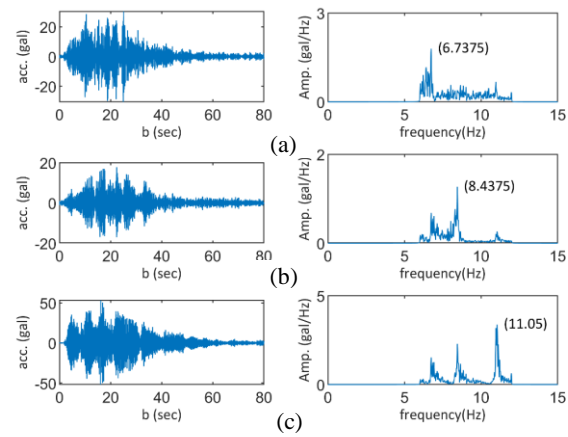


Fig. 3 The identified modal responses and spectra from responses with [6, 12]Hz

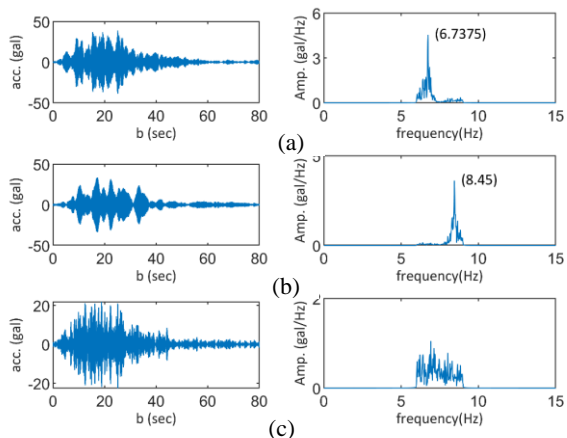


Fig. 4 The identified modal responses and spectra from responses with [6, 9]Hz

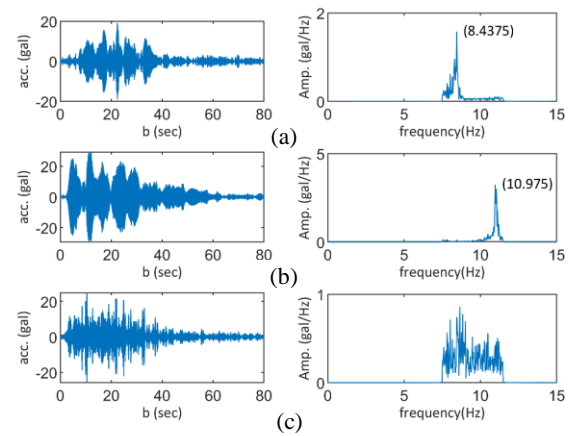


Fig. 5 The identified modal responses and spectra from responses with [7.5, 11.5]Hz

Table 1 summarizes the identified modal parameters of the six-story shear building, and the theoretical natural frequencies and modal damping ratios are also given in parentheses. These results disclose that the proposed approach with appropriate Shannon wavelets is able to accurately identify the modal vectors with MAC values larger than 0.9 and natural frequencies with differences less than 5% from the true ones. The identified damping ratios show reasonable agreement with true ones.



Table 1 Identified modal parameters for a six-story shear building under earthquake

Band-pass filtering (Hz)	Mode	MAC	Natural frequency (Hz)	Modal damping ratio (%)
[1, 6]	1	0.996	1.37 (1.31)	4.36 (3.04)
	2	0.917	3.37 (3.35)	1.46 (1.19)
	3	0.991	5.27 (5.25)	0.74 (0.76)
[6, 9]	4	0.954	6.73 (6.78)	0.44 (0.59)
	5	0.998	8.45 (8.42)	0.59 (0.47)
[7.5, 11.5]	5	0.987	8.42 (8.42)	0.87 (0.47)
	6	0.999	11.02 (11.02)	0.45 (0.36)

4. Application to Shaking Table Tests

To demonstrate the applicability of the present approach to real measured data, it is further employed to process the measured acceleration responses of a benchmark eight-story symmetric steel frame in shaking table tests (Fig. 6), which were conducted by the National Center for Research on Earthquake Engineering in Taiwan. The eight-story steel frame was 1.5m in length, 1.1m in width and 9.44m in height. Lead blocks of 250 kg were piled on each floor, such that the total mass of each floor was approximately 325 kg. The columns had H-shaped sections (H100×100×7.5×7.5). The frame was subjected to base excitations of reduced Chi-Chi earthquake in long-span direction. Figure 7 depicts the base excitations, measured acceleration responses of the 1st, 6th and 8th floors and their Fourier spectra. Notably, there are abnormal sharp peaks round 30 and 48 Hz in the spectrum of base excitations. The spectra provide rough estimation of natural frequencies of the first seven modes, which is very helpful in selecting the filtering bands in the following analyses for identifying modal parameters of the frame.

Autoregressive with exogenous input (ARX) models with the continuous Cauchy wavelet transform [20] were also employed to find the modal parameters of the frame from the measured base excitations and acceleration responses of all the floors. The identified natural frequencies and modal damping ratios are given in parentheses in Table 2, and the identified modal shapes are displayed in Fig. 8. Eight modes with the largest natural frequency of 42.41 Hz were identified even though the 8th mode was hardly excited.

Instead of considering full measurements in establishing ARX models, the present approach was applied to process the measured acceleration responses of the 1st, 6th and 8th floors. Using Shannon wavelets with $(F_c, F_b) = (4.5, 7), (10, 10), (15, 10), (28, 16)$ and $(41, 8)$ to perform the CWT and processing the resulting responses in wavelet domain yield the possible modal responses and their Fourier spectra. Figures 9 and 10 display the possible modal responses and their Fourier spectra obtained using $(F_c, F_b) = (10, 10)$ and $(28, 16)$, respectively. Each of the spectra shown in Figs. 9(a, b) and 10(a, b) has single peak and is corresponding to a real mechanical mode. Those spectra were further utilized to estimate natural frequencies and modal damping ratios, which are given in Table 2. The spectra in Figs. 9(c) and 10(c) are apparently corresponding to spurious modes. Similarly, other modal parameters, given in Table 2, were obtained from processing the wavelet transforms of responses using Shannon wavelets with $(F_c, F_b) = (4.5, 7), (15, 10)$ and $(41, 8)$. The MAC values indicate the agreement between the present modal vectors and those obtained from ARX models.



Fig. 6 A photo for an eight-story steel frame under shaking table tests

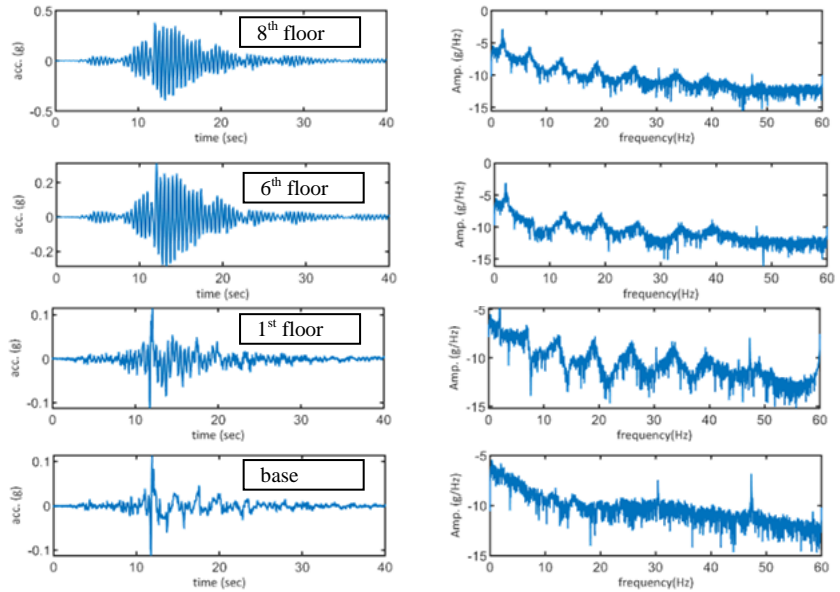


Fig. 7 Measured base excitations and the absolute accelerations responses and the corresponding spectra of 1st, 6th and 8th floors

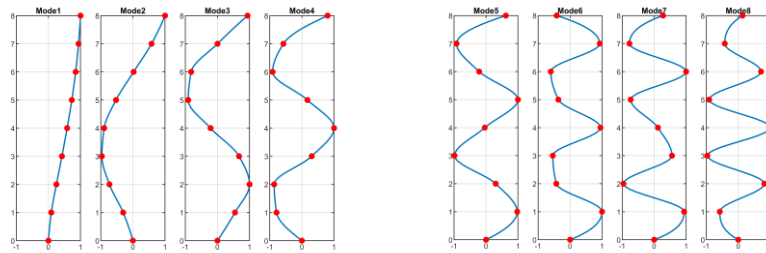


Fig. 8 Identified modal shapes by ARX

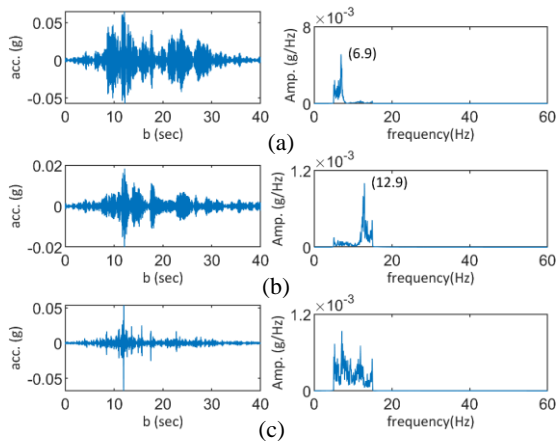


Fig. 9 The identified modal responses and spectra from responses with [5, 15]Hz of the 8-story frame

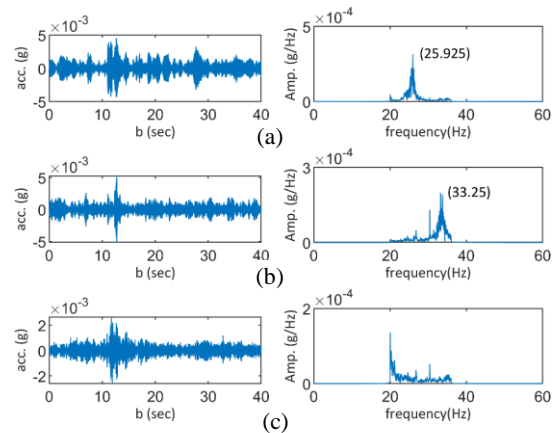


Fig. 10 The identified modal responses and spectra from responses with [20, 36]Hz of the 8-story frame



Table 2 Identified modal parameters for an eight-story steel frame under shaking table tests

Band-pass filtering (Hz)	Mode	MAC	Natural frequency (Hz)	Modal damping ratio (%)
[1, 8]	1	0.995	2.05 (2.09)	1.66 (1.18)
[5, 15]	2	0.982	6.90 (6.96)	0.69 (0.32)
	3	0.995	12.90 (12.73)	0.73 (0.54)
[10, 20]	4	0.997	19.25 (19.00)	0.46 (0.56)
[20, 36]	5	0.961	25.92 (25.78)	0.29 (0.91)
	6	0.959	33.17 (33.30)	5.0 (1.14)
[37, 45]	7	0.972	39.55 (39.06)	1.06 (1.54)

Comparisons the identified modal parameters using the present approach with those from ARX reveal that the present approach gives accurate modal vectors with MAC values larger than 0.95 and natural frequencies with less than 2% differences from those obtained from ARX. Most of the damping ratios identified by the present approach show reasonable agreement with those obtained from ARX. The modal parameters of 8th mode were not identified because the mode was hardly excited as observed from the spectra in Fig. 7.

5. Conclusion

The study has shown a valid BSS approach using the temporal predictability of wavelet transformed responses to accurately identify the modal vectors and natural frequencies of a linear system with classical damping with considering noise and underdetermined case. The study reformulates the measure of temporal predictability proposed by Stone [11, 12] in wavelet domain. The filtering property of wavelet transform allows the present approach to identify more active modes than the number of measured degrees of freedom.

The present approach was validated through processing the numerically simulated absolute acceleration responses of three degrees of freedom of a six-story shear building under earthquake with considering 10% noise. The modal vectors and natural frequencies of six modes were accurately identified, while the modal damping ratios were identified with reasonable accuracy. The identified frequencies differed from the true ones by less than 5%, whereas the MAC values were larger than 0.9. The proposed approach was further employed to handle the acceleration responses of a symmetric eight-story steel frame under shaking table tests. The modal vectors and frequencies of the first 7 modes obtained using the measured responses of three floors showed a very good agreement with the parameters identified using ARX models with complete measurements. The MAC values were larger than 0.95, while the differences were less than 2% in the natural frequencies.

6. Acknowledgements

The authors would like to thank the Ministry of Science and Technology of the Republic of China, Taiwan, for financially supporting this research under Contract No. MOST 108-221-E-009-005.

7. References

- [1] Kerschen G, Poncelet F, Golinval, J (2007): Physical interpretation of independent component analysis in structural dynamics. *Mechanical Systems and Signal Processing*, **21**, 1561–1575.



- [2] Yang YC, Nagarajaiah S (2013): Time-frequency blind source separation using independent component analysis for output-only modal identification of highly damped structures. *Journal of Structural Engineering*, ASCE, **139**(10), 1780-1793.
- [3] Hwang JS, Noh JT, Lee SH (2019): Experimental verification of modal identification of a high-rise building using independent component analysis. *International Journal of Concrete Structures and Materials*, **13**(1), doi:10.1186/s40069-018-0319-7.
- [4] Hazra B, Sadhu A, Roffel AJ, Narasimhan S (2012): Hybrid time-frequency blind source separation towards ambient system identification. *Computer-Aided Civil and Infrastructure Engineering*, **27**(5), 314-332.
- [5] Morovati V, Kazemi MT (2016): Detection of sudden structural damage using blind source separation and time-frequency approaches. *Smart Materials and Structures*, **25**(5), doi:10.1088/0964-1726/25/5/055008.
- [6] Brewick PT, Smyth AW (2017): Increasing the efficiency and efficacy of second-order blind identification (SOBI) methods. *Structural Control and Health Monitoring*, **24**, (doi: 10.1002/stc.1921)
- [7] Jin Y, Qin S, Guo J, Zhu C (2016): Output-only modal identification based on hierarchical Hough transform. *Journal of Mechanical Science and Technology*, **30**(7), 2941-2951.
- [8] Yao XJ, Yi TH, Qu CX, Li HN (2018): Blind modal identification in frequency domain using independent component analysis for high damping structures with classical damping. *Computer-Aided Civil and Infrastructure Engineering*, **33**, 35–50.
- [9] Hyvärinen A, Oja E (2000): Independent component analysis: algorithm and applications. *Neural Networks*, **13**, 411-430.
- [10] Poncelet F, Kerschen G, Golinval JC, Verhelst D (2007): Output-only modal analysis using blind source separation techniques. *Mechanical Systems and Signal Processing*, **21**, 2335–2358.
- [11] Musafere F, Sadhu A, Liu K (2016): Towards damage detection using blind source separation integrated with time-varying auto-regressive modeling. *Smart Materials and Structures*, **25**(1), doi:10.1088/0964-1726/25/1/015013
- [12] McNeill SI (2011): An analytic formulation for blind modal identification. *Journal of Vibration and Control*, **18**(14), 2111-2121.
- [13] Hazra B, Narasimhan S (2010): Wavelet-based blind identification of the UCLA Factor building using ambient and earthquake responses. *Smart Materials and Structures*, **19**(2), 1-10.
- [14] Yang YC, Nagarajaiah S (2013b): Output-only modal identification with limited sensors using sparse component analysis. *Journal of Sound and Vibration*, **332**(19), 4741–4765.
- [15] Amini F, Hedayati Y (2016): Underdetermined blind modal identification of structures by earthquake and ambient vibration measurements via sparse component analysis. *Journal of Sound and Vibration*, **366**, 117–132.
- [16] Stone JV (2001): Blind source separation using temporal predictability. *Neural Computation*, **13**, 1559–1574.
- [17] Stone JV (2002): Blind deconvolution using temporal predictability. *Neurocomputing*, **49**, 79–86.
- [18] Yang YC, Nagarajaiah S (2013): Blind modal identification of output-only structures in time-domain based on complexity pursuit. *Earthquake Engineering & Structural Dynamics*, **42**, 1885-1905.
- [19] Allemang RL, Brown DL (1983): A correlation coefficient for modal vector analysis. *Proceedings of the 1st International Modal Analysis Conference*, Bethel, Connecticut, U.S.A., 110-116.
- [20] Huang CS, Liu CY, Su WC (2016): Application of Cauchy wavelet transformation to identify time-variant modal parameters of structures. *Mechanical Systems and Signal Processing*, **80**(1), 302-323.